

conversion has been achieved with a range of 1460–1640 nm, giving a bandwidth of 180 nm. A four-wave-mixing conversion efficiency of -20 dB is achieved within a 70 nm tuning range within a 3.9 dB fluctuation. An OSNR of 30 dB is also realized within the same tuning range.

REFERENCES

1. S.L. Danielsen, P.B. Hansen, and K.E. Stubkjaer, Wavelength conversion in optical packet switching, *J Lightwave Technol* 16 (1998), 2095–2107.
2. S.J.B. Yoo, Wavelength conversion technologies for WDM network applications, *J Lightwave Technol* 14 (1996), 955–966.
3. P.V. Mamyshev, All-optical data regeneration based on self-phase modulation effect, In: *Proceedings of the 24th European Conference on Optical Communication*, 1998, pp. 475–476.
4. W. Wang, H.N. Poulsen, L. Rau, H.F. Chou, J.E. Bowers, and D.J. Blumenthal, Raman-enhanced regenerative ultrafast all-optical fiber XPM wavelength converter, *J Lightwave Technol* 23 (2005), 1105–1115.
5. C. Porzi, A. Bogoni, L. Poti, and G. Contestabile, Polarization and wavelength-independent time-division demultiplexing based on copolarized-pumps FWM in an SOA, *IEEE Photon Technol Lett* 17 (2005), 633–635.
6. J. Zhou, N. Park, J.W. Dawson, K.J. Vahala, M.A. Newkirk, and B.I. Miller, Efficiency of broadband four-wave mixing wavelength conversion using semiconductor traveling wave amplifiers, *IEEE Photon Technol Lett* 6 (1994), 50–52.
7. Z.G. Lu, J.R. Liu, S. Taebi, Y. Song, X.P. Zhang, and T. Hall, Ultra-broadband wavelength conversion system by using photonic crystal fiber, *Proc SPIE* 6781 (2007), 1L-1–1L-5.
8. Y.P. Yatsenko, A.F. Kosolapov, A.E. Levchenko, S.L. Semjonov, and E.M. Dianov, Broadband wavelength conversion in a germanosilicate-core photonic crystal fiber, *Opt Lett* 34 (2009), 2581–2583.
9. K.K. Chow, M.W.K. Mak, C. Shu, and H.K. Tsang, Widely tunable all-optical wavelength converter using a fiber ring cavity incorporating a semiconductor optical amplifier, *Opt Commun* 203 (2002), 101–106.
10. K.K. Chow, C. Shu, M.W.K. Mak, and H.K. Tsang, Widely tunable wavelength converter using double ring fiber laser with a semiconductor optical amplifier, *IEEE Photon Technol Lett* 14 (2002), 1445–1447.
11. J.H. Han, Four-wave mixing in intra-cavity dual-wavelength fiber ring laser, *Electron Lett* 47 (2011), 612–614.
12. N.A. Awang, H. Ahmad, A.A. Latif, M.Z. Zulkifli, Z.A. Ghani, and S.W. Harun, Wavelength conversion based on FWM in a HNLF by using a tunable dual-wavelength erbium doped fiber laser source, *J Modern Opt* 58 (2011), 566–572.
13. K. Inoue, Four wave mixing in an optical fiber in the zero-dispersion wavelength region, *J Lightwave Technol* 10 (1992), 1553–1561.

© 2012 Wiley Periodicals, Inc.

HIGH-ISOLATION 2.4/5.2/5.8 GHZ WLAN MIMO ANTENNA ARRAY FOR LAPTOP COMPUTER APPLICATION

Kin-Lu Wong, Huan-Jynu Jiang, and Yeh-Chun Kao
Department of Electrical Engineering, National Sun Yat-Sen University, Kaohsiung 804, Taiwan; Corresponding author: wongkl@ema.ee.nsysu.edu.tw

Received 18 May 2012

ABSTRACT: An isolation technique for two small-size tri-band wireless wide area network (WLAN) multiple-input multiple-output (MIMO) laptop computer antennas covering the 2.4/5.2/5.8 GHz bands is

presented. The proposed WLAN MIMO antennas have measured isolation of better than -21 dB in the 2.4 GHz band and -32 dB in the 5.2/5.8 GHz bands in this study. In addition to enhanced isolation achieved, good antenna efficiencies of better than about 70 and 90%, respectively, in the 2.4 GHz and 5.2/5.8 GHz bands are obtained for the two antennas. The WLAN MIMO antenna array having a planar structure of size 9×55 mm² is to be mounted at the top edge of the supporting metal plate of the laptop display. The two antennas can be fabricated at low cost on a thin FR4 substrate and are of a simple structure comprising a driven strip and a shorted strip, which provides two wide operating bands to cover the 2.4 and 5.2/5.8 GHz bands. Between the two antennas, there is an isolation element formed by a protruded ground plane and a spiral open slot embedded therein. The isolation element leads to enhanced isolation between the antennas in the 2.4/5.2/5.8 GHz WLAN bands and good antenna efficiencies for the antennas as well. Details of the isolation technique for the WLAN MIMO antennas are described, and the obtained results are presented and discussed. © 2012 Wiley Periodicals, Inc. *Microwave Opt Technol Lett* 55:382–387, 2012; View this article online at wileyonlinelibrary.com. DOI 10.1002/mop.27279

Key words: mobile antennas; wireless wide area network antennas; antenna isolation; multiple-input multiple-output antennas; laptop computer antennas

1. INTRODUCTION

The 2.4/5.2/5.8 GHz tri-band WLAN (wireless wide area network) MIMO (multiple-input multiple-output) operation [1] has been demanded to achieve enhanced signal transmission and reception for mobile communications. For laptop computer applications, the WLAN MIMO operation requires a compact WLAN antenna array having enhanced isolation between the antennas and good radiation efficiencies for the antennas as well. The isolation techniques that have been reported for related applications include the use of a T-shaped ground plane between the antennas [2–6], a neutralization line connected between the antennas [7, 8], a ground wall and a connecting line added between the antennas [9], two planar inverted-F antennas with their shorting strips or plates oriented to face each other [10, 11], slot resonators embedded in the ground plane between the antennas to decrease the effects of the excited surface currents flowing from one port to another [12–14], and so on. However, the WLAN antennas applied in these studies may not be compact or suitable for the internal laptop computer antenna applications or the applied isolation techniques are not promising to achieve improved isolation in multiple operating bands.

Recently, to achieve enhanced isolation in the 2.4/5.2/5.8 GHz WLAN bands, the technique of applying a dual-band strip resonator disposed between two WLAN laptop computer antennas to trap the near-field radiation from one antenna to another has been reported [15]. The applied dual-band strip resonator can achieve isolation (S_{21}) better than -18 dB over the 2.4/5.2/5.8 GHz bands for the two WLAN antennas. To achieve a much enhanced isolation in the 2.4/5.2/5.8 GHz WLAN bands, we present in this article a new isolation technique of using an isolation element formed by a protruded ground plane and a spiral open slot embedded therein for a high-isolation WLAN MIMO antenna array. The measured isolation between antennas for the WLAN MIMO antenna array is better than -21 dB in the 2.4 GHz band and -32 dB in the 5.2/5.8 GHz bands in this study. In addition to much enhanced isolation between antennas, good antenna efficiencies of better than about 70 and 90%, respectively, in the 2.4 and 5.2/5.8 GHz bands are obtained for the two antennas. The proposed antenna array has a planar structure

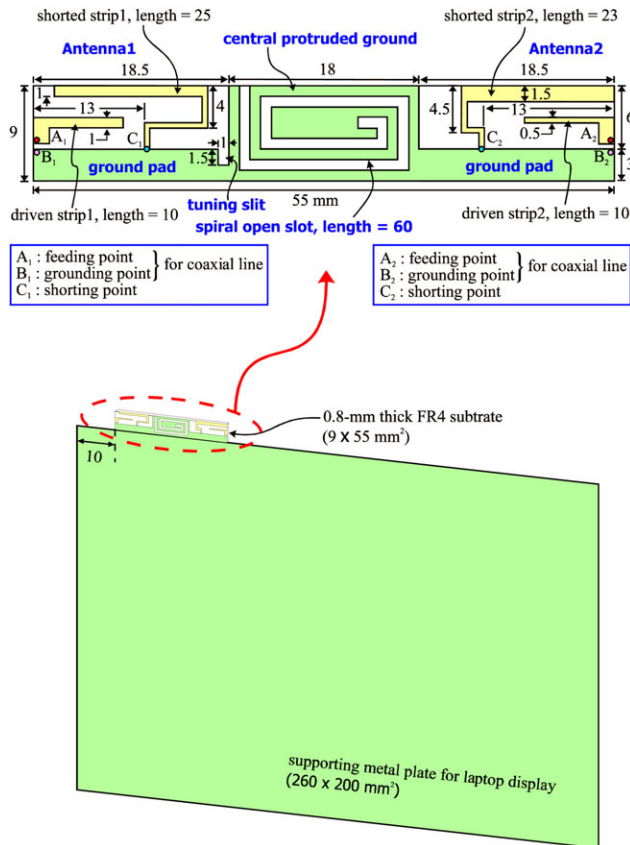


Figure 1 Geometry of the high-isolation WLAN MIMO laptop computer antenna array with an isolation element formed by a protruded ground plane and a spiral open slot embedded therein. [Color figure can be viewed in the online issue, which is available at wileyonlinelibrary.com]

of size $9 \times 55 \text{ mm}^2$ and is suitable to be mounted at the top edge of the supporting metal plate of the laptop display. Details of the proposed WLAN MIMO antenna array are described, and operating principle of the applied isolation technique is addressed. The obtained results are presented and discussed.

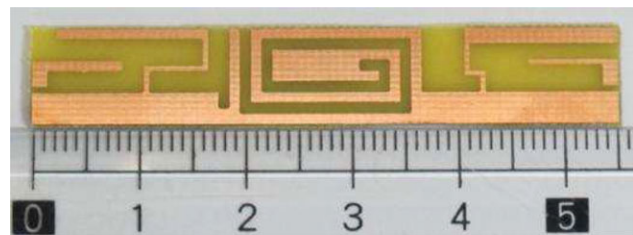
2. PROPOSED WLAN MIMO ANTENNA ARRAY

Figure 1 shows the geometry of the high-isolation WLAN MIMO laptop computer antenna array with an isolation element formed by a protruded ground plane and a spiral open slot embedded therein. The antenna array [a photo of the fabricated prototype is shown in Figure 2(a)] is mounted at the top edge of the supporting metal plate of the laptop display. The dimensions of the supporting metal plate are $260 \times 200 \text{ mm}^2$, which is a reasonable size of the laptop computer equipped with a 13-inch display panel. In the experiment, the supporting metal plate is fabricated from a 0.2-mm thick copper plate as seen in Figure 2(b).

The WLAN antenna array has a planar structure and is printed on a 0.8-mm thick FR4 substrate of size $9 \times 55 \text{ mm}^2$, relative permittivity 4.4, and loss tangent 0.024. The two antennas (antenna1 and antenna2) have a similar geometry of a driven strip and a shorted strip. The antennas have a wide lower band to cover the 2.4 GHz WLAN operation (2400~2848 MHz) and a wide upper band to cover the 5.2/5.8 GHz WLAN operation (5150~5350/5725~5875 MHz). The 2.4 GHz band is formed by a quarter-wavelength resonant mode generated by the shorted strip. The 5.2/5.8 GHz bands are formed by a quarter-wavelength resonant mode generated by the driven strip and a higher order reso-

nant mode generated by the shorted strip. Both the two antennas occupy a small size and can be disposed in a small clearance region of $6 \times 18.5 \text{ mm}^2$. Each antenna is connected to a 50- Ω coaxial line [see Fig. 2(b)], with the central connector and outer grounding sheath of the coaxial line, respectively, connected to point A_1 (A_2) and B_1 (B_2). Note that there is a ground pad of width 3 mm in the antenna array, and the ground pad is connected to the top edge of the supporting metal plate in the study. The ground pad makes it convenient to mount the WLAN antenna array at the top edge of the supporting metal plate. Also, note that the dimensions of the two antennas are slightly different from each other, which is owing to the different locations of the two antennas at the top edge of the supporting metal plate and hence the dimensions of the antennas are required to be fine adjusted such that good impedance matching for both antennas in the desired 2.4/5.2/5.8 GHz WLAN bands is obtained.

To enhance the isolation between the two antennas, an isolation element formed by a central protruded ground and a spiral open slot embedded therein is proposed. The central protruded ground can lead to improved isolation between the two antennas in the 5.2/5.8 GHz bands. The behavior is similar to that used in Ref. 16 for the LTE (long-term evolution) MIMO array in the mobile handset in which it is helpful to improve the isolation between two LTE antennas. Some isolation improvement in the 5.2/5.8 GHz bands can be achieved owing to the protruded ground in-between the two antennas. This behavior is mainly because the protruded ground can direct some excited surface currents in the ground pad toward the top edge of the protruded ground and hence decrease the excited surface currents flowing from one antenna to another. Improved isolation can thus be



(a)



(b)

Figure 2 (a) Photo of the fabricated WLAN MIMO antenna array. (b) Photo of the antenna array mounted at the top edge of the supporting metal plate for the laptop display. [Color figure can be viewed in the online issue, which is available at wileyonlinelibrary.com]

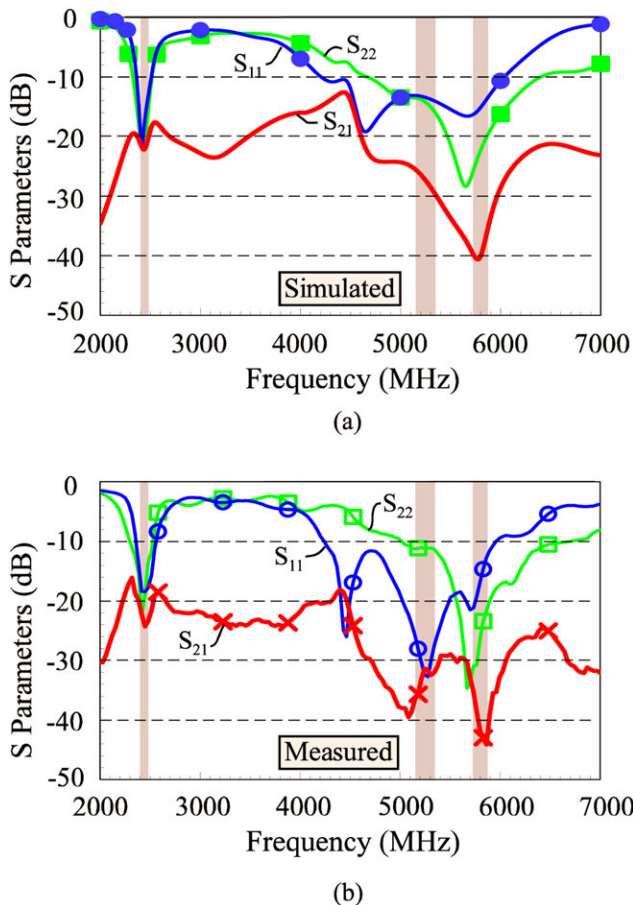


Figure 3 (a) Measured and (b) simulated S parameters of the proposed WLAN MIMO antenna array mounted at the top edge of the supporting metal plate as shown in Fig. 1. [Color figure can be viewed in the online issue, which is available at wileyonlinelibrary.com]

obtained, although the improvement isolation is about 6 dB only (from about -15 to -21 dB in the 5.2/5.8 GHz bands in this study). However, in the 2.4 GHz band, the protruded ground shows no effects on improving the isolation between the two antennas.

By embedding a spiral open slot of length 60 mm, about half-wavelength at about 2.45 GHz, in the protruded ground, enhanced isolation between the antennas in the 2.4 GHz band can be achieved. This behavior is owing to the spiral open slot acted as a resonator [17, 18] at about 2.45 GHz, which effectively traps the excited surface currents flowing in the ground pad for frequencies in the 2.4 GHz band. Hence, decrease coupling (measured S_{21} less than -21 dB in the 2.4 GHz band) between the antennas can be obtained. Further, in the 5.2/5.8 GHz bands, the spiral open slot can also be a resonant element to effectively trap the excited surface currents in the ground pad. By incorporating a small tuning slit of length 1.5 mm to fine adjust the isolation effect of the protruded ground, much enhanced isolation (measured S_{21} less than -32 dB in the 5.2/5.8 GHz bands) between the antennas in the 5.2/5.8 GHz can be obtained. That is, the proposed isolation element can lead to a high-isolation 2.4/5.2/5.8 GHz WLAN MIMO antenna array.

3. RESULTS OF THE WLAN MIMO ANTENNA ARRAY

The proposed WLAN MIMO antenna array was fabricated and tested. Figure 3 shows the measured and simulated S parameters

of the antenna array mounted at the top edge of the supporting metal plate as shown in Figure 1. The simulated results of S_{11} , S_{22} , and S_{21} obtained using the three-dimensional full-wave electromagnetic field simulator HFSS version 14 [19] are presented in Figure 3(a), while the measured data are shown in Figure 3(b). The simulated results generally agree with the measured data. Based on the bandwidth definition of 10-dB return loss, the operating bandwidths of antenna1 and antenna2 cover the 2.4 GHz and 5.2/5.8 GHz WLAN bands. The measured isolation (S_{21}) in the 2.4 GHz band is better than -21 dB. In the 5.2 and 5.8 GHz bands, the isolation is seen to be better than -32 and -34 dB, respectively.

To analyze the isolation effects, the simulated electric-field distributions in the open slot and the surface current distributions in the protruded ground plane at 2442, 5250, and 5800 MHz are shown in Figures 4(a) and 4(b). The results are obtained for antenna1 being excited. At 2442 MHz, the results indicate that the spiral open slot is at resonance [20] and trap the excited surface currents flowing from antenna1 to antenna2. This leads to very weak surface currents at the feeding point of antenna2, and hence enhanced isolation between the two antennas is obtained. Also, strong surface currents in the shorted strip of antenna1 are seen, which confirms that the 2.4 GHz band is mainly contributed by the quarter-wavelength resonant mode of the shorted strip. While at 5250 MHz, center frequency of the 5.2 GHz band, strong surface currents in the driven strip are seen, which suggests that the 5.2 GHz band is contributed by the quarter-wavelength resonant mode of the driven strip. In the 5.2 GHz band, the isolation improvements are also seen to be related to the spiral open slot trapping the excited surface currents flowing from antenna1 to antenna2.

As for operating at 5800 MHz, the driven strip and the shorted strip in its higher order resonant mode are seen to be excited. For the isolation improvement in the 5.8 GHz band, it is seen to be mainly owing to the narrow strip, which is adjacent to the tuning slit and the spiral open slot, trapping the excited surface currents flowing from antenna1 to antenna2. Note that the narrow strip is formed owing to the spiral open slot embedded in the protruded ground plane. Very weak surface currents near the feeding port of antenna2 are seen. This behavior results in a very good isolation of about -40 dB as seen in Figure 3(a). It should also be noted that the isolation in the 5.8 GHz band and the 5.2 GHz band as well can be fine adjusted by selecting a proper length of the tuning slit to effectively trap the surface currents flowing from antenna1 to antenna2 [Fig. 4(b)]. Effects of the tuning slit on the isolation between antennas are presented in Figure 5, in which the simulated S_{21} for the tuning-slit length t varied from 0 to 3 mm is shown. It is seen that the isolation in the 2.4 GHz band is generally not affected. While in the 5.2/5.8 GHz band, the isolation can be effectively fine adjusted by the tuning slit.

Effects of the spiral open slot are analyzed with the aid of Figure 6. The simulated S parameters for the slot lengths of 55 and 50 mm are, respectively, shown in Figures 6(a) and 6(b). As the isolation over the 2.4 GHz band is mainly owing to the spiral open slot acting as a resonator to trap the excited surface currents, the length of the spiral open slot is important and can be adjusted to control the isolation level for frequencies in the 2.4 GHz band. When the slot length decreases, as seen in the figure, the dip of the isolation (S_{21}) curve near the 2.4 GHz band is shifted to higher frequencies. Also, the isolation in the 5.2/5.8 GHz bands is affected. This behavior indicates that the spiral open slot also contributes a higher order resonance to decrease the isolation in the 5.2/5.8 GHz bands. This higher

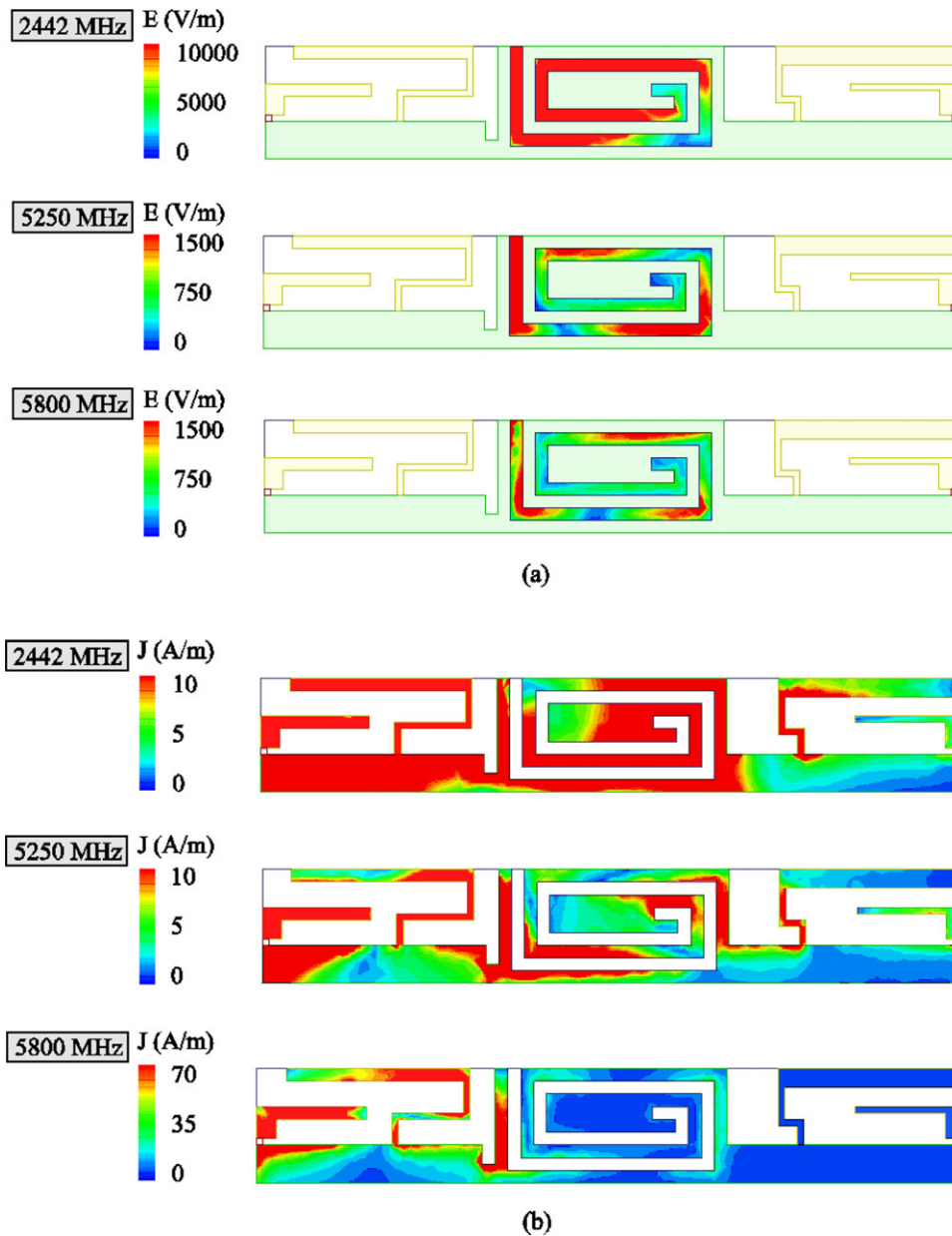


Figure 4 (a) Simulated electric-field distributions in the open slot and (b) surface current distributions in the protruded ground plane at 2442, 5250, and 5800 MHz. [Color figure can be viewed in the online issue, which is available at wileyonlinelibrary.com]

order resonance is also shifted to higher frequencies when the slot length decreases. In the proposed design, the length of the spiral open slot is selected to be 60 mm (results shown in Fig. 3), which shows good isolation results for frequencies over the 2.4/5.2/5.8 GHz bands.

More isolation analysis is conducted with the aid of Figure 7, in which the simulated S parameters for the case without the protruded ground plane, the case with the protruded ground plane only, and the case with the protruded ground plane and the spiral open slot therein (no tuning slit in the ground pad) are presented. In Figure 7(a), when there is no protruded ground plane, the S_{21} is only about -15 , -15 , and -14 dB in the 2.4, 5.2, and 5.8 GHz bands. With the presence of the protruded ground only [Fig. 7(b)], no effects on the S_{21} in the 2.4 GHz band are seen and the S_{21} is decreased to be about -20 and -22 dB in the 5.2 and 5.8 GHz bands. In Figure 7(c), it shows

that when the protruded ground plane and the spiral open slot therein are present, the S_{21} is decreased to be less than -20 , -24 , and -32 dB in the 2.4, 5.2, and 5.8 GHz bands, respectively. By further using a tuning slit (that is, the proposed design) to fine adjust the S_{21} in the 5.2/5.8 GHz bands, the S_{21} can be less than -26 and -35 dB in the 5.2 and 5.8 GHz bands, respectively (Fig. 5). Note that from the measured data shown in Figure 3, the S_{21} is less than -21 , -32 , and -34 dB in the 2.4, 5.2, and 5.8 GHz bands, respectively.

Measured radiation characteristics of the proposed WLAN MIMO antenna array were also measured. Figure 8 shows the measured antenna efficiency of the antenna array. The antenna efficiency includes the mismatching loss of the antenna. Results show that in the 2.4 GHz band, the antenna efficiency is better than about 62%. While in the 5.2/5.8 GHz bands, the antenna efficiency is better than about 82%. The measured

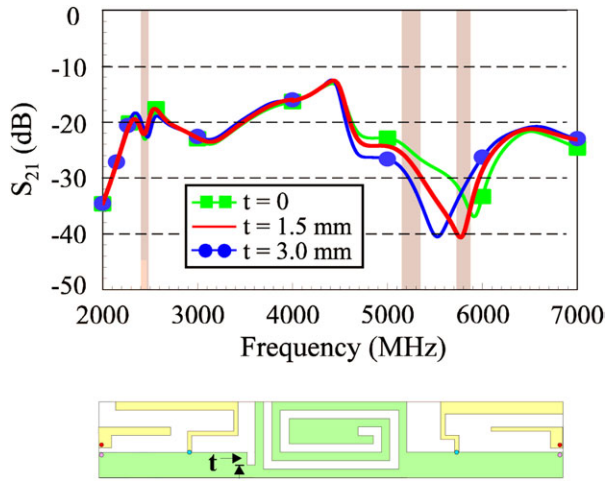


Figure 5 Simulated S_{21} as a function of the tuning-slit length t . Other parameters are the same as in Fig. 1. [Color figure can be viewed in the online issue, which is available at wileyonlinelibrary.com]

three-dimensional total-power radiation patterns of the antenna array at 2442, 5250, and 5800 MHz are shown in Figure 9. The radiation patterns are shown in their front views, that is, the observers seeing into the $-x$ direction. Stronger radiation is seen

in the $-y$ direction for antenna1 at all frequencies. This is mainly because antenna1 is disposed near the right corner of the top edge and backed by the protruded ground. For antenna2, stronger radiation is seen in the $+y$ direction at 2442 MHz. For higher frequencies at 5250 and 5800 MHz, the radiation is less asymmetric as seen at 2442 MHz or the corresponding frequencies of antenna1. This radiation characteristic is related to antenna2 disposed in the inner side of the antenna array and its

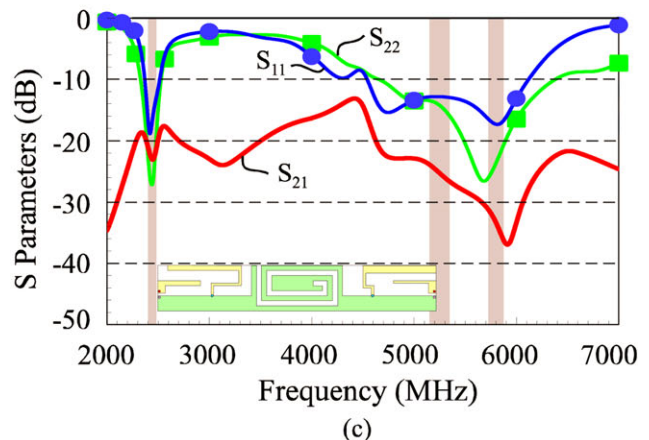
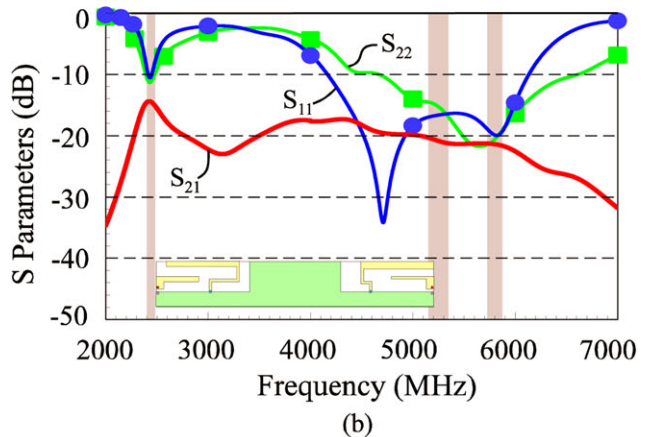
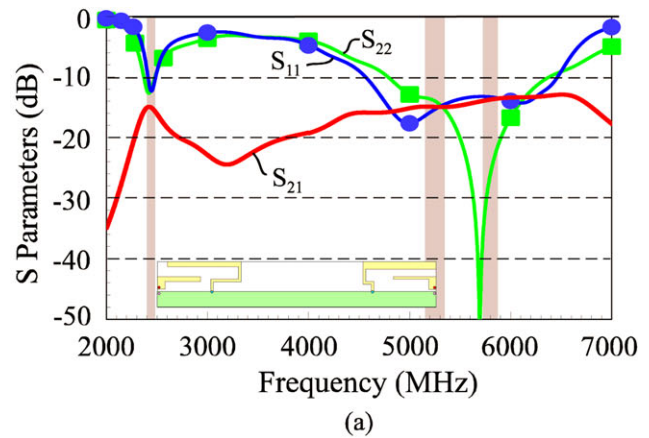


Figure 7 Simulated S parameters for (a) the case without the protruded ground plane, (b) the case with the protruded ground plane only, and (c) the case with the protruded ground plane and the spiral open slot therein (no tuning slit in the ground pad). [Color figure can be viewed in the online issue, which is available at wileyonlinelibrary.com]

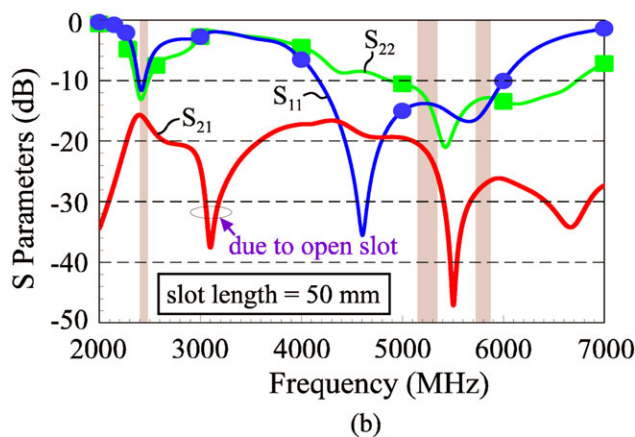
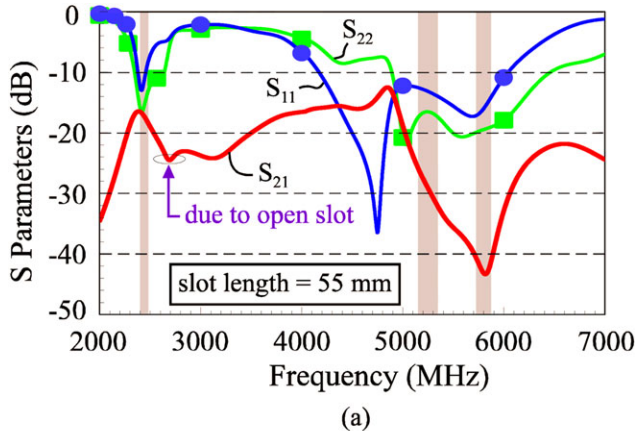


Figure 6 Simulated S parameters for different lengths of the spiral open slot in protruded ground plane. (a) Slot length = 55 mm. (b) Slot length = 50 mm. [Color figure can be viewed in the online issue, which is available at wileyonlinelibrary.com]

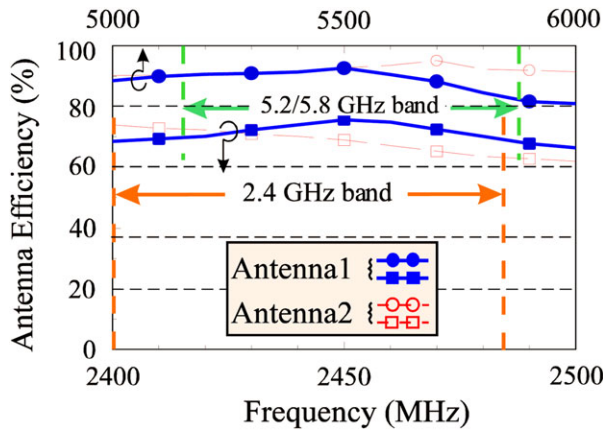


Figure 8 Measured antenna efficiency (mismatching loss included) of the proposed WLAN MIMO antenna array. [Color figure can be viewed in the online issue, which is available at wileyonlinelibrary.com]

relative location along the top edge of the supporting metal plate. By moving the antenna array along the top edge of the supporting metal plate, it is expected that some variations in the radiation patterns of antenna1 and antenna2 as compared to those shown in Figure 9 will be seen.

4. CONCLUSION

A high-isolation 2.4/5.2/5.8 GHz triband WLAN MIMO antenna array for laptop computer applications has been proposed. A new isolation element formed by a central protruded ground and a spiral open slot embedded therein have been shown to effectively enhance the isolation between the antennas in the proposed antenna array. Experimental results showed that the isolation between antennas can be better than -21 , -32 , and -34 dB in the 2.4, 5.2, and 5.8 GHz bands, respectively. The operating principle of the proposed antenna array has also been ana-

lyzed in detail. The proposed WLAN MIMO antenna array also has attractive properties of small size and planar structure, which makes it very promising for applications in the slim laptop computers with a thin profile.

REFERENCES

1. N. Olano, C. Charlie, K. Ishimiya, and Z. Ying, WLAN MIMO throughout test in reverberation chamber, In: IEEE AP-S International Symposium, San Diego, CA, 2008, pp. 1–4.
2. T.Y. Wu, S.T. Fang, and K.L. Wong, Printed diversity monopole antenna for WLAN operation, *Electron Lett* 38 (2002), 1625–1626.
3. T.Y. Wu, S.T. Fang, and K.L. Wong, Printed diversity dual-band monopole antenna for WLAN operation, *Microwave Opt Technol Lett* 36 (2003), 436–439.
4. G. Chi, B. Li, and D. Qi, Dual-band printed diversity antenna for 2.4/5.2-GHz WLAN application, *Microwave Opt Technol Lett* 45 (2005), 561–563.
5. K.L. Wong, S.W. Su, and Y.L. Kuo, Printed ultra-wideband diversity monopole antenna, *Microwave Opt Technol Lett* 38 (2003), 257–259.
6. K.L. Wong, C.H. Chang, B. Chen, and S. Yang, Three-antenna MIMO system for WLAN operation in a PDA phone, *Microwave Opt Technol Lett* 48 (2006), 1238–1242.
7. A. Chebihi, C. Luxey, A. Diallo, P.L. Thuc, and R. Staraj, A novel isolation technique for closely spaced PIFAs for UMTS mobile phones, *IEEE Antennas Wireless Propag Lett* 7 (2008), 665–668.
8. J. Rohola and J. Ollikainen, Analysis of isolation of two-port antenna systems using simultaneous matching, In: European Conference on Antennas and Propagation (EuCAP), Edinburgh, UK, 2007, pp. 1–5.
9. K. Chung and J.H. Yoon, Integrated MIMO antenna with high isolation characteristic, *Electron Lett* 43 (2007), 199–201.
10. K.L. Wong, A.C. Chen, and Y.L. Kuo, Diversity metal-plate PIFA for WLAN operation, *Electron Lett* 39 (2003), 590–591.
11. K.L. Wong, Y.Y. Chen, S.W. Su, and Y.L. Kuo, Diversity dual-band planar inverted-F antenna for WLAN operation, *Microwave Opt Technol Lett* 38 (2003), 223–225.
12. M. Karaboikis, C. Soras, G. Tsachtsiris, and V. Makios, Compact dual-printed inverted-F antenna diversity systems for portable wireless devices, *IEEE Antennas Wireless Propag* 3 (2004), 9–14.
13. G.A. Mavridis, J.N. Sahalos, and M.T. Chryssomallis, Spatial diversity two-branch antenna for wireless devices, *Electron Lett* 42 (2006), 266–268.
14. K.J. Kim and K.H. Ahn, The high isolation dual-band inverted F antenna diversity system with the small N-section resonators on the ground plane, *Microwave Opt Technol Lett* 49 (2007), 731–734.
15. T.W. Kang and K.L. Wong, Isolation improvement of 2.4/5.2/5.8 GHz WLAN internal laptop computer antennas using dual-band strip resonator as a wavetrap, *Microwave Opt Technol Lett* 52 (2010), 58–64.
16. K.L. Wong, T.W. Kang, and M.F. Tu, Antenna array for LTE/WWAN and LTE MIMO operations in the mobile phone, *Microwave Opt Technol Lett* 53 (2011), 1569–1573.
17. K.L. Wong, Y.W. Chang, and S.C. Chen, Bandwidth enhancement of small-size WWAN tablet computer antenna using a parallel-resonant spiral slit, *IEEE Trans Antennas Propag* 60 (2012), 1705–1711.
18. C.T. Lee and K.L. Wong, Uniplanar printed coupled-fed PIFA with a band-notching slit for WLAN/WiMAX operation in the laptop computer, *IEEE Trans Antennas Propag* 57 (2009), 1252–1258.
19. Available at: <http://www.ansys.com/products/hf/hfss/>, ANSYS HFSS, Ansoft Corp., Pittsburg, PA 15219.
20. K.L. Wong and F.H. Chu, Internal planar WWAN laptop computer antenna using monopole slot elements, *Microwave Opt Technol Lett* 51 (2009), 1274–1279.

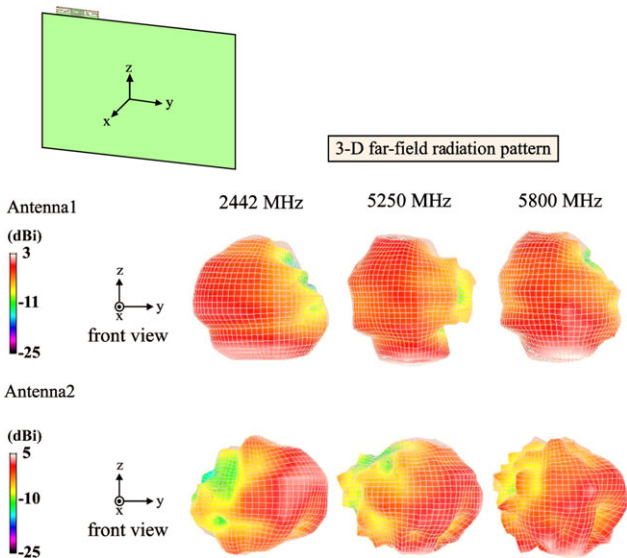


Figure 9 Measured three-dimensional total-power radiation patterns of the proposed WLAN MIMO antenna array at 2442, 5250, and 5800 MHz. [Color figure can be viewed in the online issue, which is available at wileyonlinelibrary.com]